Polímeros
ISSN 1678-5169 (Online)

https://doi.org/10.1590/0104-1428.20240020

ORIGINAL ARTICLES

Biodegradable hybrid PLA composites incorporating coffee husks and mineral fillers

Riquelme Gomes da Silva[1], Laysa Silva Barboza[1], Pedro Henrique Poubel Mendonça da Silveira[1,2], Marceli do Nascimento da Conceição[3], Roberto Carlos da Conceição Ribeiro[3] and Daniele Cruz Bastos[1]*

[1]Faculdade de Ciências Exatas e Engenharias, Universidade do Estado do Rio de Janeiro – UERJ, Rio de Janeiro, RJ, Brasil

[2]Programa de Pós-graduação em Ciência e Engenharia de Materiais, Instituto Militar de Engenharia – IME, Rio de Janeiro, RJ, Brasil

[3]Coordenação de Rochas Ornamentais, Centro de Tecnologia Mineral – CETEM, Rio de Janeiro, RJ, Brasil

**daniele.bastos@uerj.br*

Abstract

This article details the development of hybrid composites with a PLA matrix filled with coffee husks, potassium feldspar, and Bahia Beige marble. Comprehensive analysis included FTIR, hardness, contact angle, density tests, SEM for microstructural insights, and XRF for optimizing raw material compositions. Also, variance analysis was applied in all results. The study revealed that these biodegradable composites hold promise for sustainable applications. Density variations were noted due to particle compaction, and hardness slightly decreased with coffee husks, attributed to uneven component distribution. Increased hydrophilicity was observed with filler addition. SEM confirmed strong interfacial adhesion, and color consistency was maintained. Notably, coffee husks significantly enhanced the degradation rate of PLA, achieving a 100% higher rate compared to pure PLA. The presence of calcium and potassium minerals offers additional benefits for soil health. The study suggests that thermoformed, multi-layered composite capsules can be fully biodegradable, promoting environmental sustainability in coffee capsule production.

Keywords: *biodegradability, poly(lactic acid), polymer composite sustentability.*

How to cite: Silva, R. G., Barboza, L. S., Silveira, P. H. P. M., Conceição, M. N., Ribeiro, R. C. C., & Bastos, D. C. (2024). Biodegradable hybrid PLA composites incorporating coffee husks and mineral fillers. *Polímeros: Ciência e Tecnologia*, *34*(3), e20240031. https://doi.org/10.1590/0104-1428.20240020

1. Introduction

Coffee husks among the most consumed beverages worldwide, offering a wide range of products and consumption opportunities. Over the past decades, coffee has evolved from a simple commodity into a specialized product, ushering in a new era of consumption where quality, flavor, and aesthetics are the primary aspects sought after in the quest for the perfect brew. With advancements in technology, new methods of coffee preparation have emerged, including the popular coffee capsule, which enables the rapid and convenient production of hot coffee[1,2].

However, the rapid growth in coffee capsule consumption has given rise to a series of environmental issues stemming from improper disposal of these capsules. Coffee capsules are composed of a mixture of materials, including plastics, aluminum, paper, and organic materials, which pose significant recycling challenges. In Brazil, despite the potential capacity to recycle 60% to 75% of these capsules, the actual return rate is only 11%[3,4]. These environmental concerns have compelled coffee companies to implement alternative recycling programs, with industry leaders such as Nespresso establishing numerous collection points for used capsules. Nonetheless, a substantial portion of these capsules often ends up in landfills after the aluminum is recovered for recycling purposes.

Plastic capsules are primarily made from polypropylene (PP), a low-cost material typically combined with ethylene vinyl alcohol and coated with a layer of aluminum/polyethylene to enhance oxygen barrier properties. This packaging plays a crucial role in preserving the aroma of coffee during its storage period, minimizing the loss of highly volatile compounds and the ingress of oxygen[5-7]. To address environmental concerns, the use of biodegradable plastics in specific applications, such as soil cover films, trash bags, and disposable packaging, has been proposed as an advancement in the field of bioeconomic, reducing the carbon footprint. A notable example of a bioplastic that is both renewable-based and biodegradable is polylactic acid (PLA)[8-13].

However, PLA exhibits some limitations compared to petroleum-derived plastics, such as low thermal stability and inadequate barrier properties, particularly in high-temperature environments. To overcome these challenges, researchers have explored the development of composites

and nanocomposites using biodegradable polymers like PLA, reinforced with materials from renewable sources. Additionally, hybrid composites have been developed by blending natural, synthetic, or a combination of fibers in a single matrix to enhance the physical, mechanical, and thermal properties of these materials[14-16]. The hybridization of high-aspect-ratio fibers with low-aspect-ratio particulate mineral fillers is an established industrial technique for minimizing anisotropic effects, with common examples of low-aspect-ratio particulate fillers used to modify thermoplastics including calcium carbonate, talc, mica, and glass beads[16-21].

Furthermore, coffee husks, representing 12% to 18% of the dry weight of a coffee cherry, contain significant quantities of carbohydrates, fibers (cellulose, hemicellulose, and lignin), and proteins[22]. They are considered renewable, biodegradable materials and have a lower environmental impact when compared to synthetic fibers. These components are akin to those found in most lignocellulosic fillers used in the production of polymer-based composites, making coffee husks a promising alternative to conventionally employed materials[23-25]. Simultaneously, stone processing industries generate solid waste and stone slurry during their dimensioning process, which often ends up in landfills or other disposal sites, causing significant environmental impacts[16,26-28].

In this context, the novelty of this study is the production of biodegradable hybrid PLA composites PLA as a matrix incorporating coffee husks waste and minerals rich in potassium and calcium. These composites have the potential to be utilized in food packaging materials, such as coffee capsules, providing an eco-friendly alternative to conventional options. Additionally, recycled minerals could be employed as soil seedling fixatives and as sources for releasing micronutrients. This research aims to contribute to environmental sustainability and foster innovative solutions in the food and packaging industries.

2. Materials and Methods

2.1 Raw materials

The PLA used in this work as a polymeric matrix was purchased from Minnesota (USA, grade 2003D, Mn 88,500 Da and Mw/Mn 1.8; density 1.24 $g.cm^{-3}$, and used as received, in pellet form. The organic waste, Arabic coffee husks (CH), with density of 1.4554 ± 0.0007 $g.cm^{-3}$, were provided by the company Unique Cafés Especiais (São Lourenço, MG, Brazil). Coffee husks were ground with industrial knives to a particle size of less than 2 mm. The mineral samples were donated by CETEM (Rio de Janeiro, Brazil). To enrich the composite with calcium, waste from the cutting of Bahia beige marble (BB), with density of 2.832 ± 0.0005 $g.cm^{-3}$ (Ourolândia, Bahia), was used, with granulometry of less than 20 μm. Also, potassium from a potassium feldspar (PF) (Serra Negra, Sergipe, Brazil), with granulometry of less than 20 μm and density of 2.8608 ± 0.0015 $g.cm^{-3}$, was used.

2.2 Composites processing

The materials were previously dried in an oven with forced air circulation at 100 °C until constant weight for 24 h, and stored in a desiccator for another 24 h before processing. The materials were mixed manually, and the composites were compounded with PLA/coffee husks/potassium feldspar/Bahia beige marble. (PLA/CH/PF/BB) in different proportions, as described in Table 1. Each formulation was fed into a twin-screw extruder (TeckTril, DCT model, L/D=40, D=20) equipped with ten heating zones, ranging from 95 to 190 °C, from the feed to die, and rotating at 47 rpm. The specimens for characterization were obtained by pressing 10 g of pelletized samples from the extrusion at a temperature of 190 °C for 300 s, with pressure of 70 KPa for film formation, and then cooled in a cold press for 60 s.

2.3 Characterization: raw material

The mineralogical composition of Bahia beige, potassium feldspar and coffee husks were evaluated by the X-Ray fluorescence (XRF). This analysis was carried out with an Axios Max Panalytical (WDS-2) spectrometer operating at 4 kW. The calcination loss was determined with a Leco TGA-701 thermogravimetric analyzer with two heating ramps, one from 25-107 °C at 10 °C/min and the second from 107-1000 °C at 40 °C/min. The test ended after three identical sequential weights.

2.4 Characterization: composite

The morphological analysis (SEM) of raw materials and processed composites was conducted using a Tescan Vega 3 microscope. The samples were previously cryogenically fractured into transverse sections and then coated with gold in a sputtering chamber. Images were obtained using an electron beam power of 15kV and magnifications of 200 and 1500x.

Fourier-transform infrared spectra were acquired using a Nicolet 6700 FTIR spectrometer (Thermo Scientific). The samples were mounted on an attenuated total reflectance (ATR) accessory equipped with a ZnSe crystal prior to scanning. The spectra were obtained with an accumulation

Table 1. Composition and nomenclature of composites formulations.

Groups	PLA (wt.%)	CH (wt.%)	PF (wt.%)	BB (wt.%)
100/0/0/0	100	-	-	-
80/10/5/5	80	10	5	5
70/20/5/5	70	20	5	5
60/30/5/5	60	30	5	5
50/40/5/5	50	40	5	5

PLA = Poly(lactic acid); CH = coffee husks; PF = potassium feldspar; BB = Bahia beige.

of 120 scans. Density analyses were conducted at 23 °C following the guidelines of ASTM D792[29]. A Gehaka DSL910 densimeter was employed. Five samples for accurate density determination represented each group. The Shore D hardness tests were conducted in accordance with ASTM D2240-15[30], utilizing a GS-702 durometer. The arithmetic mean of five measurements was calculated for each sample. The wettability of the materials surface was examined through water contact angle measurements using a Ramé-Hart NRL A-100-00 goniometer. The evolution of the droplet shape was recorded with a CCD camera every 10 s for a period of 90 s for each sample, at room temperature.

A spectrophotometer (Delta Vista 450G) was used to measure the color parameters of the specimens using a high-efficiency LED source and D65, A, C and F7 illuminants at 10º angle and 16 mm aperture. The color measurement of PLA and composites was performed according to the CIElab method (Commission Internationale de L'Eclairage) which allows obtaining the parameters L*, referring to luminosity, which varies from black (0) to white (100); a*, which is the intensity of the red(+)/green(-) color; and b*, the intensity of the yellow(+)/blue(-) color[26]. Laboratory-accelerated soil degradation studies were conducted at 25 °C in microbially active soil beds (garden soil with 2% humus content, 22-24% water, pH 5.6, stored in glass containers). PLA and composite samples (mass 0.322-0.340 g and thickness 0.8-1.1 mm) were removed from containers, washed with distilled water, cleaned by sonication, dried and weighed. Aliquots of the acid solution were collected to monitor the levels of potassium and calcium by inductively coupled plasma (ICP) analysis, initially and after 30 days.

2.5 Variance analysis (ANOVA)

Variance analysis (ANOVA) was applied in all results to verify, with a 95% confidence level, any significant differences between the averages. In positive cases, the mean values of the results were then compared using the Tukey's test, also called honestly significant difference (HSD). This is calculated by Equation 1, in which "q" is a tabulated constant, "EMS" is the error mean square and "r" is the repetitions number for each condition [31].

$$HSD = q\sqrt{\frac{EMS}{r}} \quad (1)$$

3. Results and Discussions

3.1 XRF results

Table 2 provides the results of XRF analysis for samples of coffee husk, potassium feldspar, and Bahia Beige marble. The following data reveal information about the chemical composition of these samples. XRF analysis of Bahia Beige, as shown in Table 2, indicated that calcium constitutes approximately one third of the total sample composition, also accounting for about 47 wt.% during calcination, which is related to carbonates. This result suggests that the material naturally occurs in the form of calcium carbonate, known as calcite.

Table 2. Chemical composition (wt.%) of the raw materials used, as determined by XRF.

OXIDE	CH	PF	BB
MgO	0.46	2.2	6.05
Al_2O_3	0.60	14.3	0.48
SiO_2	2.00	62.6	4.50
P_2O_5	0.49	0.51	-
SO_3	0.24	0.15	-
K_2O	4.30	4.00	-
CaO	0.83	4.90	45.70
TiO_2	< 0.10	1.40	-
MnO	-	0.10	-
Fe_2O_3	0.66	6.90	0.16
SrO	-	< 0.10	-
Bi_2O_3	-	< 0.10	-
Co_3O_4	< 0.10	-	-
Na_2O	0.11	2.5	-
NiO	< 0.10	-	-
Rb_2O	-	< 0.10	-
WO_3	0,22	-	-
ZrO_2	-	< 0.10	-
LOI	89.9	0.34	43.15

CH = coffee husks; PF = potassium feldspar; BB = Bahia beige.

As for potassium feldspar, which is used as a source of potassium, the analysis revealed that it contains approximately 4 wt.% K_2O and 62.6 wt.% SiO_2 in its composition. These values are consistent with the use of this mineral as a source of potassium in various applications. Coffee husks, on the other hand, exhibit a composition characterized by a high concentration of carbon, accounting for 90 wt.% of the sample. Additionally, the analysis reveals that they contain approximately 2 wt.% of SiO_2 and 4.30 wt.% of K_2O. The presence of 0.83 wt.% of CaO contributes to the overall structure of the husks. The high value of Loss on Ignition (LOI) of 89.9 wt.% is indicative of typical thermal decomposition of organic materials[32].

Regarding potassium feldspar, its composition is marked by a high concentration of SiO_2 at 62.6%. Other significant oxides include Al_2O_3 and K_2O, representing 14.30 and 4.00 wt.%, respectively. Oxides such as Fe_2O_3 and CaO are also present, with fractions of 6.90 and 4.90 wt.%, respectively. Other oxides, such as Na_2O, are found in smaller quantities. The LOI of 0.34 wt.% is attributable to the ceramic characteristics of potassium feldspar.

3.2 FTIR results

Figure 1 shows the FTIR-ATR spectra of coffee husk, potassium feldspar and bahia beige raw materials.

Figure 1 presents the FTIR spectra of the starting materials in the range of 500 to 4000 cm^{-1}, encompassing all relevant absorption bands. In the infrared spectrum of potassium feldspar, a series of overlapping bands between 650 and 1000 cm^{-1} are prominent. The absorption band in the region of 1250 to 830 cm^{-1} can be attributed to the asymmetric stretching vibration of Si-O groups, with a peak maximum at 998 cm^{-1}, the symmetric stretching at 800 and 780 cm^{-1}, and the symmetric and asymmetric bending modes

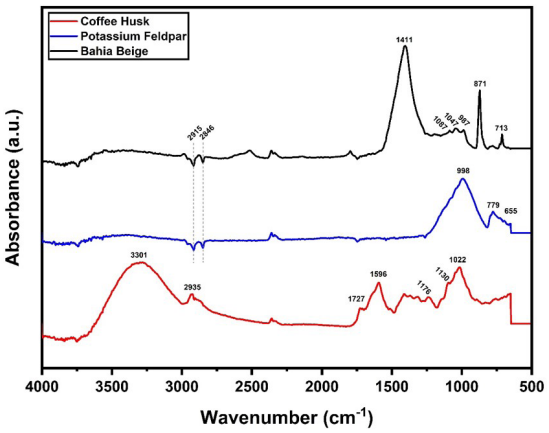

Figure 1. FTIR spectra of coffee husk, potassium feldspar and bahia beige.

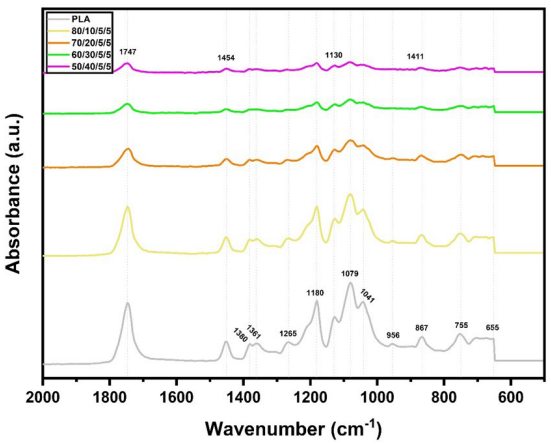

Figure 2. FTIR spectra of PLA and PLA composites.

of Si-O at 650 cm^{-1}, respectively[33,34]. The bands found at 2846 and 2915 cm^{-1}, both in potassium feldspar and bahia beige, are related to the vibrations corresponding to CH_2 and CH_3, and have been previously recorded in polypropylene composites reinforced with bahia beige. The peak at 987 and 1047 cm^{-1} corresponds to C=C bending, while the peak at 1081 cm^{-1} corresponds to C-O stretching. These three bands are commonly found in marbles[35].

The obtained infrared spectrum for coffee husk exhibits similarities with previously documented records in literature[36,37]. The analysis has revealed the presence of absorption peaks attributable to various chemical compounds, such as caffeine, carbohydrates, and proteins, all of which have been previously explored in publications related to the coffee theme. The spectral range situated between 3600 and 3000 cm^{-1} reflects the presence of water and the presence of OH (hydroxyl) groups on the surface of coffee husk, with a peak observed at 3301 cm^{-1}. Such behavior is reported by Marchi et al.[38] for epoxy matrix composites reinforced with ubim fibers (*Geonoma Baculífera*), but it occurs generally in all lignocellulosic fibers. The peak located at 2935 cm^{-1} is associated with the presence of lignocellulosic components, such as in coffee husk[39]. Caffeine also exhibits characteristic absorptions in the spectral regions of 1731 and 1596 cm^{-1}. It is noteworthy that wavenumbers in the range of 1700-1600 cm^{-1} have a known correlation with the concentration of chlorogenic acid in coffee samples, as discussed by Capek et al.[40]. In addition to these observations, notable absorbance peaks were detected at 1241, 1014, and 771 cm^{-1}, which may be associated with components such as sucrose in the 1242-1218 cm^{-1} range, and arabinogalactans at 1065-1020 cm^{-1} [41-43]. Table 3 summarizes the absorption bands related to the functional groups of each of the reinforcement materials used.

FTIR spectra of PLA showed characteristic absorption bands of asymmetric and symmetric C=O and C-O 1747 and 1079 cm^{-1}, respectively (Figure 2). A peak found at 1747 cm^{-1} in PLA is related to C=O stretching. The addition of coffee husk may contain functional groups capable of forming hydrogen bonds with the carbonyl group of PLA. These hydrogen bonds can modify the molecular structure of PLA,

Table 3. Absorption Bands of Coffee Husk, Potassium Feldspar, and Bahia Beige.

Material	Absorption Range	Functional Group/ Vibration
Coffee Husk	3600-3000	O-H; Water
Coffee Husk	2935	Caffeine
Coffee Husk	1731, 1596	Caffeine
Coffee Husk	1700-1600	Chlorogenic acid
Coffee Husk	1241	Sucrose
Coffee Husk	1014	Arabinogalactans
Coffee Husk	771	Arabinogalactans
Potassium Feldspar	1250-830	Asymmetric stretching of Si-O
Potassium Feldspar	998	Asymmetric stretching of Si-O
Potassium Feldspar	800, 780	Asymmetric stretching of Si-O
Potassium Feldspar	655	Symmetric and asymmetric bending of Si-O
Potassium Feldspar	2846, 2915	CH_2 and CH_3 vibrations
Bahia Beige	2846, 2915	CH_2 and CH_3 vibrations
Bahia Beige	987, 1047	C=C bending
Bahia Beige	1081	C-O stretching

altering the spectroscopic characteristics of the C = O band, consequently reducing its intensity in the composites[44]. Such behavior is also observed in the peaks at 1380 and 1349 cm^{-1} of PLA, where these peaks represent C-H stretching. These peaks lost intensity with the addition of coffee husk. The bands at 867 and 755 cm^{-1}, were attributed to the crystal and amorphous phases of neat[45,46]. The infrared bands of BB displayed results consistent with the characteristic bands of limestone, namely 1454 - 1380/867 - 755 cm^{-1} (carbonate ion stretching). The composites exhibited a physical interface as no changes were observed in the infrared peaks[47,48]. A decrease at peak strength occurred with increasing amount of natural fiber in composites, suggesting physical interaction. Table 4 summarizes the absorption bands found in PLA and the composites, along with their relationship with the functional groups present in each band.

3.3 Density, hardness, and contact angle results

Table 5 presents the results obtained in the density, hardness, and contact angle tests.

The results obtained for the studied composites were compared with the values of the traditional coffee capsule made of Polypropylene (PP) found in the market. The density values of the composites ranged from 1.138 to 1.259 g/cm^3, with density decreasing as the filler content in the composites increased. Similar density results were found by Chagas et al.[16] when studying hybrid thermoplastic composites based on polypropylene with additions of Bahia Beige and coconut fiber. In their study, the authors found density values ranging from 0.829 to 1.146 g/cm^3. Density variations are attributed to differences in particle compaction and particle wall roughness[49,50].

Table 4. Absorption Bands of PLA and Composites.

Material	Absorption Range	Functional Group/Vibration
PLA	1747	C=O stretching
PLA	1079	C-O stretching
PLA	1380, 1349	C-H stretching
PLA	867, 755	Crystalline and amorphous phases
Composites	1746	C=O stretching (reduced)
Composites	1380, 1349	C-H stretching (reduced)
Composites	1454	Carbonate ion stretching
Composites	867-755	Carbonate ion stretching

Table 5. Results of density, hardness and contact angle of formulations.

Groups	Density (g/cm^3)	Hardness (Shore D)	Contact angle (º)
Capsule	0.866 ± 0.019	80.67 ± 0.58	74.61 ± 0.29
100/0/0/0	1.259 ± 0.025	78.67 ± 2.30	74.80 ± 0.17
80/10/5/5	1.190 ± 0.045	78.67 ± 2.08	64.25 ± 3.48
70/20/5/5	1.200 ± 0.005	74.33 ± 9.07	76.70 ± 3.75
60/30/5/5	1,166 ± 0.005	71.33 ± 2.51	65.85 ± 0.76
50/40/5/5	1.138 ± 0.090	69.33 ± 2.31	64.02 ± 0.55

Capsule = traditional coffee capsule made of PP.

Based on the density results presented in Table 5, Table 6 provides the analysis of variance for the density values of the composites.

The equality hypothesis, with a confidence level of 95%, was confirmed as the calculated F value was lower than the tabulated Fc value. This indicates that there was no significant difference in the inclusion of coffee husk, potassium feldspar, and bahia beige reinforcements in the PLA matrix. For a more detailed analysis, a comparison of means was conducted using the Tukey test, as shown in Table 7.

From the results of the Tukey test, it is observed that groups A and B are statistically different from group C, as they do not share the same letter designation for a certain statistical equality. Within groups A and B, there are no significant differences in mean density, as they share the same letter designation. However, group B contains various compositions of PLA and coffee husk, with slightly decreasing densities as the percentage of coffee husk increases. This trend indicates that the incorporation of coffee husk affects the density of the composite materials. This Tukey analysis is conducted as a complementary approach to ANOVA, as it allows for the comparison of means and, based on the minimum significant difference, determines statistical equality/difference from this difference in mean values. However, this increase will exert little influence in practical applications such as coffee capsules. The low density inherent to plastic materials renders them advantageous in applications where weight reduction is imperative, particularly in industries such as packing, automotive and aerospace.

The results of the Shore D hardness test showed that the hardness of the coffee capsules is higher than that of PLA and the composites. The capsules exhibited hardness values of 80.67 Shore D, while PLA had an average value of 78.67 Shore D. The addition of 10 wt.% coffee husk did not result in changes in the hardness of the composite, remaining the same as PLA. Additions of 20, 30, and 40 wt.% coffee husk, combined with potassium feldspar and Bahia beige, led to a reduction in the hardness of the hybrid composites due to the possible uneven distribution of reinforcements in the polymer matrix. The increase in filler content in the matrix decreases the hardness of the composite, as the interaction of

Table 6. ANOVA results for the density of Coffee Capsule and the studied composites.

	Degree Freedom	Sum of Squares	Mean Square	F Value	Prob>F
Treatment	5	0.28	0.056	29.74	2.30202E-6
Residue	12	0.02	0.002		
Total	17	0.30			

Table 7. Comparison of means by Tukey test for the density values of the composites and coffee capsule.

	Mean	Groups		
PLA	1.25933	A		
70/20/5/5	1.20033	A	B	
80/10/5/5	1.19	A	B	
60/30/5/5	1.16633	A	B	
50/40/5/5	1.138		B	
Coffee Capsule	0.871			C

Table 8. ANOVA results for the hardness of Coffee Capsule and the studied composites.

	Degree Freedom	Sum of Squares	Mean Square	F Value	Prob>F
Treatment	5	310.50	62.10	3.58	0.03255
Residue	12	208.00	17.33		
Total	17	518.50			

polymer molecules is hindered, mainly due to the presence of organic fibers from coffee husks that are further away from the PLA chains. However, the incorporation of these organic reinforcements at high levels facilitates the degradation of the composites in agricultural soils, as expected, since the aim is to facilitate biodegradation[16,51,52].

Table 8 provides the ANOVA results for the hardness values of the composites.

The equality hypothesis, with a confidence level of 95%, was confirmed as the calculated F value was lower than the tabulated Fc value. This indicates that there was no significant difference in the inclusion of coffee husk, potassium feldspar, and bahia beige reinforcements in the PLA matrix. The mean comparison of hardness values by Tukey test is shown in Table 9.

The results of the Tukey Test indicate that all analyzed conditions have very similar means. The grouping designation "A" suggests that there are no statistically significant differences between the means of these groups. The decrease in hardness of PLA and composites compared to the coffee capsule is not very significant when observed through statistical analysis.

The contact angle results revealed that the values obtained for PLA are consistent with those reported by Manju et al.[34], and are similar to the contact angle observed in the commercial coffee capsule. The variation in the contact angle of the composites was attributed to the rough surface texture caused by the presence of fillers. According to Kadea et al.[53], a rough surface could facilitate the diffusion of moisture or water into the material, thereby accelerating degradation. Regarding the contact angle, values below 90º were recorded, indicating the hydrophilicity of the composites, similar to the commercial capsule, that probably receive additives during processing, reducing the contact angle if compared to neat PP contact anlge. Additives can impact the biodegradability of polymers[54].

However, the addition of fillers resulted in a decrease of approximately 10º in the contact angle values, enhancing the hydrophilic characteristic. Siakeng et al.[54] demonstrated that a PLA and pineapple leaf fiber biocomposite degraded faster than pure PLA. This implies that these materials, when in contact with soil, are likely to degrade more readily, as they readily absorb water and consequently decompose more quickly, releasing micronutrients (calcium, potassium, and carbon) into the soil.

Table 10 provides the ANOVA results for the contact angle values of the composites.

The equality hypothesis, with a confidence level of 95%, was confirmed as the calculated F value was lower than the tabulated Fc value. This indicates that there was no significant difference in the inclusion of coffee husk, potassium feldspar, and bahia beige reinforcements in the PLA matrix. The mean comparison of contact angle values by Tukey test is shown in Table 11.

Table 9. Comparison of means by Tukey test for the hardness values of the composites and coffee capsule.

	Mean	Groups
Coffee Capsule	80.67	A
80/10/5/5	78.67	A
PLA	78.67	A
70/20/5/5	74.33	A
60/30/5/5	71.33	A
50/40/5/5	69.33	A

Based on the comparison of means, it is concluded that there is a statistically significant difference between groups A and B. The composites in group A tend to have higher contact angles compared to the composites in group B. This may indicate greater hydrophobicity in the composites of group A compared to those in group B. These findings are important for understanding how different composite compositions can affect surface contact properties, which may have implications in specific applications such as coatings or packaging materials.

Due to the lower water contact angle of the Biocomposites, moisture or water in the soil can more easily diffuse into the material, accelerating degradation[53].

3.4 Microstructure

Figure 3 shows the SEM micrographs of coffee husk, potassium feldspar and bahia beige.

Such findings are reported in the work of Santos et al.[47], who developed polypropylene matrix composites reinforced with Bahia Beige, obtaining a visual grain distribution similar to that presented in the current study.

The SEM micrographs of coffee husk reveal particles formed from agglomerated fibers of irregular lengths, along with some smaller particles remaining after the blade milling process. These results indicate that coffee husk exhibits a tendency to exfoliate when subjected to mechanical forces, leading to the formation of smaller fibers and particles[55]. The micrograph at 1500x magnification provides a detailed view of the surface of various coffee husk fibers, varying in shapes and sizes, that have clustered together. The rough surface displays a pattern of valleys and peaks distributed across its entire extent. This surface irregularity is particularly advantageous when seeking effective mechanical adhesion to the polymeric matrix, especially in the absence of chemical fiber treatment or the use of compatibilizing agents[56].

The SEM image of potassium feldspar reveals the particle distribution. It can be observed that smaller-sized particles tend to agglomerate, while larger-sized ones do

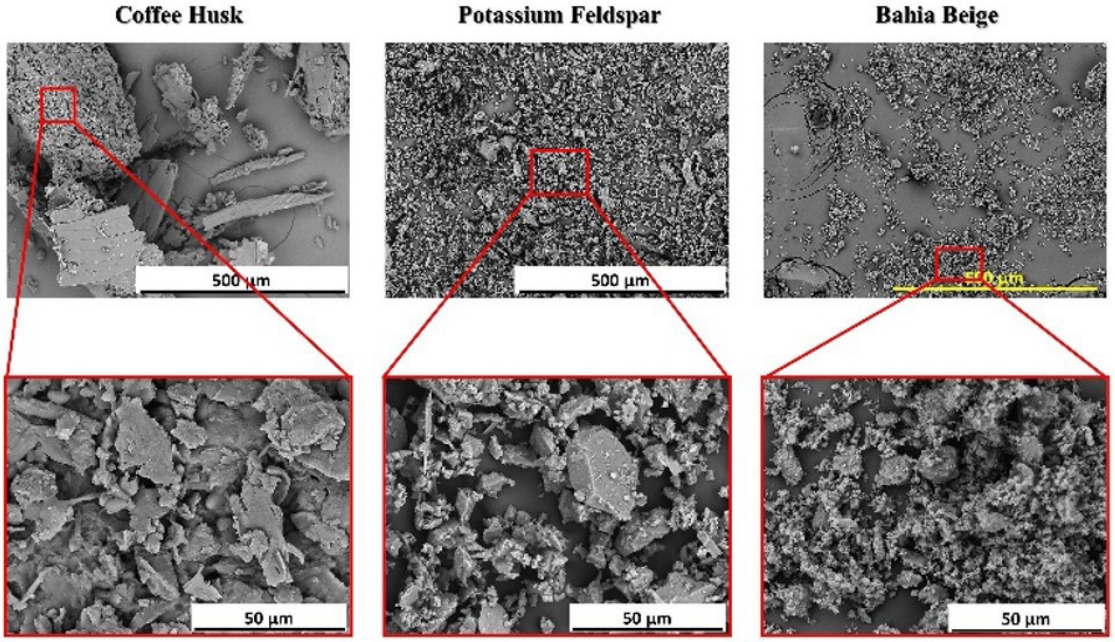

Figure 3. SEM images of the raw materials used in this study: coffee husk, potassium feldspar, and Bahia beige marble (200 and 1500 x magnification).

Table 10. ANOVA results for the contact angle of Coffee Capsule and the studied composites.

	Degree Freedom	Sum of Squares	Mean Square	F Value	Prob>F
Treatment	5	1525.67	305.13	50.68	2.25367E-17
Residue	45	270.95	6.02		
Total	50	1796.61			

not exhibit this tendency[57]. In general, potassium feldspar particles have dimensions on the order of a few tens of micrometers. The images of Bahia Beige showcase the grain morphology, highlighting an irregular distribution with the presence of larger grains, suggesting incomplete grain comminution. Figure 4 shows the fracture micrograph of the coffee capsule and the analyzed composites.

In the SEM micrograph of the coffee capsule, we observe a slightly rough surface on the polypropylene due to processing. This behavior was previously observed in the study by Silveira et al.[58], where polypropylene composites reinforced with hemp fibers functionalized with maleic anhydride were processed. The processing of the pure polymer resulted in a structure with low porosity and high uniformity, but the addition of fibers and the compatibilizing agent led to the formation of porosity.

The images of the PLA show a surface with little roughness, with some stress propagation marks in the fractured region. The addition of reinforcements increased the surface roughness of the analyzed composites. In the images of the 80/10/5/5 composite, we can observe particles attached to the material at the fracture region. This indicates good interfacial adhesion in the composite, as there was little material detachment during fracture. The increase in coffee husk concentration not only increased the roughness of the composites but also the porosity. This is evident in the images of the 70/20/5/5, 60/30/5/5, and 50/40/5/5 composites, where we can see the presence of pores.

Table 11. Comparison of means by Tukey test for the hardness values of the composites and coffee capsule.

	Mean	Groups	
70/20/5/5	76.70	A	
PLA	74.80	A	
Coffee Capsule	74.10	A	
60/30/5/5	65.85		B
80/10/5/5	64.25		B
50/40/5/5	64.02		B

3.5 Color parameters results

The color parameters in Table 12 show L*, a* and b* values of the composites. The L* values of PLA film without particles were 85.42 (D65), 85.6 (A), 85.41 (C) and 85.36 (F7).

The lightness was greater in the PLA composites with all illuminants used. The L* value decreased, because distributed

Table 12. Colorimetric parameters of PLA and composites obtained.

		PLA	80/10/5/5	70/20/5/5	60/30/5/5	50/40/5/5
D65	**L***	85.42	48.83	27.61	20.91	11.03
	a*	0.06	9.57	7.50	6.41	4.97
	b*	2.15	20.64	12.70	11.06	7.07
A	**L***	85.6	51.1	29.22	22.31	12.05
	a*	1.67	11.32	9.86	8.34	6.68
	b*	2.09	24.11	14.89	13.19	8.64
C	**L***	85.41	48.88	27.64	20.93	11.04
	a*	0.07	8.82	7.05	6.07	4.77
	b*	2.14	20.76	12.8	11.11	7.11
F7	**L***	85.36	49.16	27.73	21.01	11.06
	a*	0.13	9.48	7.37	6.19	4.76
	b*	1.97	21.16	12.85	11.20	7.11

D65 = daylight; A = incandescent light; C = diffused sunlight from a cloudy sky at noon; F7 = cool fluorescent source.

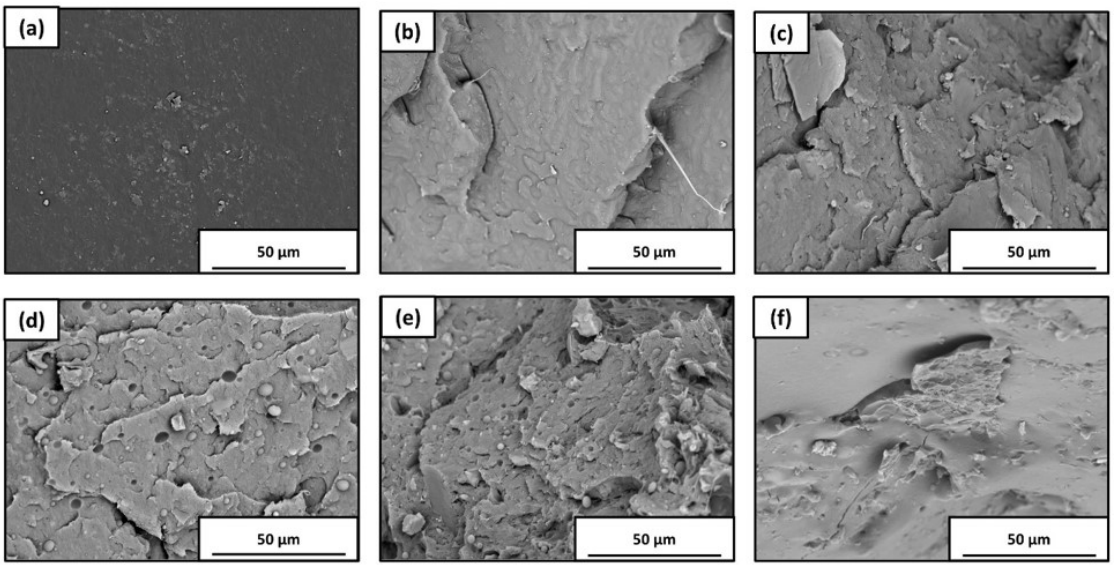

Figure 4. SEM images of the coffee capsule fracture surface (a) for comparison, pure PLA (b), and the processed composites: 80/10/5/5 (c); 70/20/5/5 (d); 60/30/5/5 (e); (f) 50/40/5/5.

particles act as a light barrier in PLA composite films, as shown in the SEM image in Figure 4. The morphology of composites can be explained by the good distribution of particles in the PLA matrix. The PLA composites had a light brown color because a* and b* values increased compared to pure PLA, which is related to the increased amount of coffee husks. The analysis of samples using different illuminants (D65, A, C and F) enabled evaluating variations in the color of the material under routine daily conditions.

The morphology of composites can significantly influence the results of a colorimetric analysis in various ways. The distribution, size, and shape of the filler particles affect color uniformity, light reflection, and absorption. Rougher or more complex surfaces can diffuse light differently, altering the perception of color. The opacity and transparency of the composite, influenced by particle concentration, also impact color intensity and hue. The color of the filler particles directly modifies the final color of the material, and internal light reflection can intensify certain colors or cause iridescence[59]. Color consistency pertains to the extent to which the color of a product or material remains uniform across different batches, manufacturing runs, or viewing conditions. It denotes the degree of adherence to a specified standard or reference in terms of color accuracy over time and under varying circumstances. Maintaining color consistency is imperative in numerous industries, including packing, printing, textiles, and cosmetics, to ensure that products consistently meet stringent quality standards and satisfy customer expectations. Taking D65 as the standard reading, a color difference not exceeding 5 CIElab units for each parameter is acceptable, so the samples showed good color consistency[5,60].

3.6 Biodegradability results

Figure 5 shows the biodegradability results for PLA and composites.

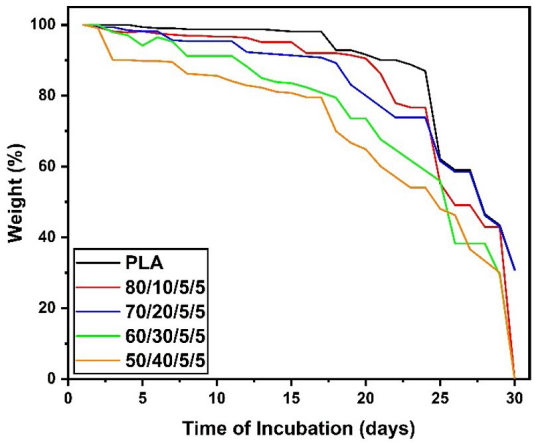

Figure 5. Biodegradability results of formulation composites.

After a 30-day incubation period at 25 °C, the PLA film deteriorated by 68.95%. Similar results were achieved by Mitchell and Hirt[61], for PLA fibers in diferente diameters (32 and 118 mm). The PLA fibers subjected to conditions of 80 °C and 100% relative humidity experienced a daily weight reduction of 2% up to day 30. On day 30, the authors related that the average weight loss reached 69% for the PLA32 samples and 65% for the PLA118 samples, respectively. According to their reults, following the 30-day degradation period, there was an insufficient amount of material remaining from either diameter for further analysis.

In our work, the addition of coffee husk resulted in an increase in the biodegradation of the composites, leading to complete degradation of the PLA composites for the 80/10/5/5, 60/30/5/5, and 50/40/5/5 composites.

According to Vasile et al.[62] and Kadea et al.[53] the degradation rate of the biocomposites in soil can be influencied by time, humidity, temperature, the soil mocroorganism, interactions between PLA and fiber, and the tickness of composite. Lignocellulosic fibers have been widely studied due to their unique properties, including biodegradability, mechanical strength, and low cost. When incorporated into plastic composite materials, these fibers can enhance the material's biodegradation, facilitating microbial decomposition and reducing environmental impact.

The 70/20/5/5 composite exhibited behavior similar to that of PLA. This demonstrates that it's possible to reduce the percentage of PLA by using waste in the formulation, which can not only decrease the price of the final product but also contribute to sustainability. Additionally, the levels of calcium and potassium increased from 200 to 800 mg/L and from 22 to 46 mg/L, respectively, after 30 days. These minerals can be used as seedling fixatives in soil and as sources of micronutrient release.

The 60/30/5/5 and 50/40/5/5 composites exhibited a higher biodegradation rate in the first 17 days. After this period, all composites showed an exponential increase in the biodegradation rate. PLA and the 70/20/5/5 composite showed less deterioration at the end of the test, with 68.95% and 69.24%, respectively. After 30 days, the 80/10/5/5, 60/30/5/5, and 50/40/5/5 composites showed a final deterioration of 100%.

4. Conclusions

In this article, we developed hybrid composites of PLA matrix filled with coffee husks, potassium feldspar, and Bahia Beige marble. We conducted a comprehensive assessment that included the analysis of the composition of the reinforcing materials, the identification of components and evaluation of chemical reactions through FTIR, and the investigation of physical and mechanical properties through hardness, contact angle, and density tests, in addition to microstructural analysis by SEM. Also, variance analysis was performed in all results.

Based on the results obtained, it is evident that biodegradable hybrid composites made from PLA exhibit significant potential for sustainable applications. The XRF analysis provided information about the composition of the raw materials, helping to optimize the compositions used in the manufacturing process of the composites. Density results showed variations due to particle compaction and particle wall roughness. Although there was a slight reduction in hardness with the addition of coffee husks, this change was attributed to the uneven distribution of components in the matrix.

Contact angle analysis demonstrated the hydrophilic nature of the composites, similar to that of commercial capsules, but the addition of fillers increased hydrophilicity. SEM images confirmed a strong interfacial adhesion of the components due to melting during processing. Furthermore, color parameters indicated consistency in coloration among the formulations.

Biodegradation tests revealed that the addition of coffee husks significantly increased the degradation rate of PLA composites. After 30 days of incubation at 25°C, the PLA film without coffee husks deteriorated by 68.94%, while composites with coffee husks showed a 100% higher degradation rate. Additionally, the presence of calcium and potassium minerals in the composites could be beneficial, as these minerals can serve as soil seedling fixatives and sources of micronutrient release.

It is important to emphasize that the final product's creation will involve several processing stages. As a result, it will be manufactured using the thermoforming process with multi-layered composite sheets, resulting in capsules with multiple layers.

These results are promising, suggesting that coffee capsules containing poly(lactic acid) enriched with coffee husks and calcium and potassium minerals can be 100% biodegradable, contributing to a reduction in environmental impact. The combination of increased hydrophilicity and an accelerated degradation rate makes these composites ideal for sustainable applications, facilitating decomposition in the soil after consumption. This study paves the way for an eco-friendlier approach to coffee capsule manufacturing and related products.

5. Author's Contribution

• **Conceptualization** – Daniele Cruz Bastos; Roberto Carlos da Conceição Ribeiro.

• **Data curation** – Pedro Henrique Poubel Mendonça da Silveira.

• **Formal analysis** – Laysa Silva Barboza.

• **Funding acquisition** – Daniele Cruz Bastos; Roberto Carlos da Conceição Ribeiro.

• **Investigation** – Riquelme Gomes da Silva; Laysa Silva Barboza.

• **Methodology** – Daniele Cruz Bastos; Roberto Carlos da Conceição Ribeiro.

• **Project administration** – Daniele Cruz Bastos; Roberto Carlos da Conceição Ribeiro.

• **Resources** – Riquelme Gomes da Silva; Laysa Silva Barboza; Pedro Henrique Poubel Mendonça da Silveira.

• **Software** – Pedro Henrique Poubel Mendonça da Silveira.

• **Supervision** – Daniele Cruz Bastos; Roberto Carlos da Conceição Ribeiro.

• **Validation** – Daniele Cruz Bastos; Roberto Carlos da Conceição Ribeiro.

• **Visualization** – Daniele Cruz Bastos; Pedro Henrique Poubel Mendonça da Silveira.

• **Writing – original draft** – Pedro Henrique Poubel Mendonça da Silveira; Marceli do Nascimento da Conceição.

• **Writing – review & editing** – Daniele Cruz Bastos; Pedro Henrique Poubel Mendonça da Silveira.

6. Acknowledgements

The authors acknowledge to CNPq, and Faperj.

7. References

1. Samoggia, A., & Busi, R. (2023). Sustainable coffee capsule consumption: understanding Italian consumers' purchasing drivers. *Frontiers in Sustainable Food Systems*, *7*, 1-13. http://doi.org/10.3389/fsufs.2023.1088877.
2. Samoggia, A., & Riedel, B. (2019). Consumers' perceptions of coffee health benefits and motives for coffee consumption and purchasing. *Nutrients*, *11*(3), 653. http://doi.org/10.3390/nu11030653. PMid:30889887.
3. Domingues, M. L. B., Bocca, J. R., Fávaro, S. L., & Radovanovic, E. (2020). Disposable coffee capsules as a source of recycled polypropylene. *Polímeros*, *30*(1), e2020009. http://doi.org/10.1590/0104-1428.05518.
4. Nanni, A., Colonna, M., & Messori, M. (2022). Fabrication and characterization of new eco-friendly composites obtained by the complete recycling of exhausted coffee capsules. *Composites Science and Technology*, *222*, 109358. http://doi.org/10.1016/j.compscitech.2022.109358.
5. Suaduang, N., Ross, S., Ross, G. M., Pratumshat, S., & Mahasaranon, S. (2019). Effect of spent coffee grounds filler on the physical and mechanical properties of poly(lactic acid) bio-composite films. *Materials Today: Proceedings*, *17*(Part 4), 2104-2110. http://doi.org/10.1016/j.matpr.2019.06.260.
6. Otoukesh, M., Vera, P., Wrona, M., Nerin, C., & Es'haghi, Z. (2020). Migration of dihydroxyalkylamines from polypropylene coffee capsules to Tenax® and coffee by salt-assisted liquid–liquid extraction and liquid chromatography-mass spectrometry. *Food Chemistry*, *321*, 126720. http://doi.org/10.1016/j.foodchem.2020.126720. PMid:32276149.
7. Cincotta, F., Tripodi, G., Merlino, M., Verzera, A., & Condurso, C. (2020). Variety and shelf-life of coffee packaged in capsules. *Lebensmittel-Wissenschaft + Technologie*, *118*, 108718. http://doi.org/10.1016/j.lwt.2019.108718.
8. Garlotta, D. (2001). A literature review of poly(lactic acid). *Journal of Polymers and the Environment*, *9*(2), 63-84. http://doi.org/10.1023/A:1020200822435.
9. Taib, N.-A. A. B., Rahman, M. R., Huda, D., Kuok, K. K., Hamdan, S., Bakri, M. K. B., Julaihi, M. R. M. B., & Khan, A. (2023). A review on poly lactic acid (PLA) as a biodegradable polymer. *Polymer Bulletin*, *80*(2), 1179-1213. http://doi.org/10.1007/s00289-022-04160-y.
10. Ashothaman, A., Sudha, J., & Senthilkumar, N. (2023). A comprehensive review on biodegradable polylactic acid polymer matrix composite material reinforced with synthetic and natural fibers. *Materials Today: Proceedings*, *80*(Part 3), 2829-2839. http://doi.org/10.1016/j.matpr.2021.07.047.
11. Swetha, T., Bora, A., Mohanrasu, K., Balaji, P., Raja, R., Ponnuchamy, K., Muthusamy, G., & Arun, A. (2023). A comprehensive review on polylactic acid (PLA): synthesis, processing and application in food packaging. *International Journal of Biological Macromolecules*, *234*, 123715. http://doi.org/10.1016/j.ijbiomac.2023.123715. PMid:36801278.
12. Wu, Y., Gao, X., Wu, J., Zhou, T., Nguyen, T. T., & Wang, Y. (2023). Biodegradable polylactic acid and its composites: Characteristics, processing, and sustainable applications in sports. *Polymers*, *15*(14), 3096. http://doi.org/10.3390/polym15143096. PMid:37514485.
13. Di Bartolo, A., Infurna, G., & Dintcheva, N. T. (2021). A review of bioplastics and their adoption in the circular economy. *Polymers*, *13*(8), 1229. http://doi.org/10.3390/polym13081229. PMid:33920269.
14. Lima, A. M., Santos, M. C. C., Bastos, D. C., Libano, E. V. D. G., & Pereira, P. S. C. (2021). Polypropylene/sugarcane bagasse composites: influence of processing. *Brazilian Journal of Development*, *7*(12), 110053-110065. http://doi.org/10.34117/bjdv7n12-002.
15. Chandgude, S., & Salunkhe, S. (2021). In state of art: mechanical behavior of natural fiber-based hybrid polymeric composites for application of automobile components. *Polymer Composites*, *42*(6), 2678-2703. http://doi.org/10.1002/pc.26045.
16. Chagas, G. N., Barros, M. M., Leão, A. G., Tapanes, N. L. C. O., Ribeiro, R. C. C., & Bastos, D. C. (2022). A hybrid green composite for automotive industry. *Polímeros*, *32*(2), e2022017. http://doi.org/10.1590/0104-1428.20220027.
17. Morelli, C. L., Pouzada, A. S., & Sousa, J. A. (2009). Influence of hybridization of glass fiber and talc on the mechanical performance of polypropylene composites. *Journal of Applied Polymer Science*, *114*(6), 3592-3601. http://doi.org/10.1002/app.30980.
18. Hashemi, S. (2008). Hybridization effect on flexural properties of single- and double-gated injection moulded acrylonitrile butadiene styrene (ABS) filled with short glass fibres and glass beads particles. *Journal of Materials Science*, *43*(14), 4811-4819. http://doi.org/10.1007/s10853-008-2683-1.
19. Carvalho, G. B., Canevarolo, S. V., Jr., & Sousa, J. A. (2020). Influence of interfacial interactions on the mechanical behavior of hybrid composites of polypropylene/short glass fibers/hollow glass beads. *Polymer Testing*, *85*, 106418. http://doi.org/10.1016/j.polymertesting.2020.106418.
20. Lapčík, L., Maňas, D., Lapčíková, B., Vašina, M., Staněk, M., Čépe, K., Vlček, J., Waters, K. E., Greenwood, R. W., & Rowson, N. A. (2018). Effect of filler particle shape on plastic-elastic mechanical behavior of high density poly(ethylene)/mica and poly(ethylene)/wollastonite composites. *Composites.*

Part B, Engineering, *141*, 92-99. http://doi.org/10.1016/j.compositesb.2017.12.035.

21. Gerardo, C. F., França, S. C. A., Santos, S. F., & Bastos, D. C. (2020). A study of recycled high-density polyethylene with mica addition: influence of mica particle size on wetting behavior, morphological, physical, and chemical properties. *International Journal of Developmental Research*, *10*(6), 37223-37228.
22. Hejna, A., Formela, K., & Saeb, M. R. (2015). Processing, mechanical and thermal behavior assessments of polycaprolactone/agricultural wastes biocomposites. *Industrial Crops and Products*, *76*, 725-733. http://doi.org/10.1016/j.indcrop.2015.07.049.
23. Sung, S. H., Chang, Y., & Han, J. (2017). Development of polylactic acid nanocomposite films reinforced with cellulose nanocrystals derived from coffee silverskin. *Carbohydrate Polymers*, *169*, 495-503. http://doi.org/10.1016/j.carbpol.2017.04.037. PMid:28504172.
24. Sanjay, M. R., Madhu, P., Jawaid, M., Senthamaraikannan, P., Senthil, S., & Pradeep, S. (2018). Characterization and properties of natural fiber polymer composites: a comprehensive review. *Journal of Cleaner Production*, *172*, 566-581. http://doi.org/10.1016/j.jclepro.2017.10.101.
25. Hejna, A. (2021). Potential applications of by-products from the coffee industry in polymer technology: current state and perspectives. *Waste Management*, *121*(3), 296-330. http://doi.org/10.1016/j.wasman.2020.12.018. PMid:33406477.
26. Sharma, R. K., Lakhani, R., & Tomar, P. (2018). A simple novel mix design method and properties assessment of foamed concretes with limestone slurry waste. *Journal of Cleaner Production*, *171*, 1650-1663. http://doi.org/10.1016/j.jclepro.2017.10.073.
27. Barros, M. M., Oliveira, M. F. L., Ribeiro, R. C. C., Bastos, D. C., & Oliveira, M. G. (2020). Ecological bricks from dimension stone waste and polyester resin. *Construction & Building Materials*, *232*, 117252. http://doi.org/10.1016/j.conbuildmat.2019.117252.
28. Malaquias, E. O., Pereira, A. A. M., Jr., Silveira, P. H. P. M., Altoé, L., & Teles, C. R. (2021). Uso de cálculo estequiométrico para avaliação da produção de biogás obtido da água residuária do café. *Brazilian Journal of Production Engineering*, *7*(2), 48-58. http://doi.org/10.47456/bjpe.v7i2.34548.
29. American Society for Testing and Materials – ASTM. (2020). ASTM D792-20: standard test methods for density and specific gravity (relative density) of plastics by displacement. West Conshohocken: ASTM.
30. American Society for Testing and Materials – ASTM. (2021). ASTM D2240-15(2021): standard test method for rubber property-durometer hardness. West Conshohocken: ASTM.
31. Ribeiro, M. P., Neuba, L. M., Silveira, P. H. P. M., Luz, F. S., Figueiredo, A. B.-H. S., Monteiro, S. N., & Moreira, M. O. (2021). Mechanical, thermal and ballistic performance of epoxy composites reinforced with *Cannabis sativa* hemp fabric. *Journal of Materials Research and Technology*, *12*, 221-233. http://doi.org/10.1016/j.jmrt.2021.02.064.
32. Acchar, W., Dultra, E. J. V., & Segadães, A. M. (2013). Untreated coffee husk ashes used as flux in ceramic tiles. *Applied Clay Science*, *75-76*, 141-147. http://doi.org/10.1016/j.clay.2013.03.009.
33. Saikia, B. J., Parthasarathy, G., & Sarmah, N. C. (2008). Fourier transform infrared spectroscopic estimation of crystallinity in SiO_2 based rocks. *Bulletin of Materials Science*, *31*(5), 775-779. http://doi.org/10.1007/s12034-008-0123-0.
34. Manju, P., Krishnan, P. S. G., & Nayak, S. K. (2021). Effect of morphology and hydroxyl groups of different nanoparticles on the properties of PLA bionanocomposites. *Materials Today: Proceedings*, *41*(Part 5), 1169-1174. http://doi.org/10.1016/j.matpr.2020.09.508.
35. Khan, A., Patidar, R., & Pappu, A. (2021). Marble waste characterization and reinforcement in low density polyethylene composites via injection moulding: towards improved mechanical strength and thermal conductivity. *Construction & Building Materials*, *269*, 121229. http://doi.org/10.1016/j.conbuildmat.2020.121229.
36. Wang, N., Fu, Y., & Lim, L. (2011). Feasibility study on chemometric discrimination of roasted Arabica coffees by solvent extraction and Fourier transform infrared spectroscopy. *Journal of Agricultural and Food Chemistry*, *59*(7), 3220-3226. http://doi.org/10.1021/jf104980d. PMid:21381653.
37. Wang, N., & Lim, L.-T. (2012). Fourier transform infrared and physicochemical analyses of roasted Coffee. *Journal of Agricultural and Food Chemistry*, *60*(21), 5446-5453. http://doi.org/10.1021/jf300348e. PMid:22563854.
38. Marchi, B. Z., Silveira, P. H. P. M., Bezerra, W. B. A., Nascimento, L. F. C., Lopes, F. P. D., Candido, V. S., Silva, A. C. R., & Monteiro, S. N. (2023). Ballistic performance, thermal and chemical characterization of ubim fiber (*Geonoma baculifera*) reinforced epoxy matrix composites. *Polymers*, *15*(15), 3220. http://doi.org/10.3390/polym15153220. PMid:37571114.
39. Reis, N., Franca, A. S., & Oliveira, L. S. (2013). Performance of diffuse reflectance infrared Fourier transform spectroscopy and chemometrics for detection of multiple adulterants in roasted and ground coffee. *Lebensmittel-Wissenschaft + Technologie*, *53*(2), 395-401. http://doi.org/10.1016/j.lwt.2013.04.008.
40. Capek, P., Paulovičová, E., Matulová, M., Mislovičová, D., Navarini, L., & Suggi-Liverani, F. (2014). Coffea arabica instant coffee: chemical view and immunomodulating properties. *Carbohydrate Polymers*, *103*, 418-426. http://doi.org/10.1016/j.carbpol.2013.12.068. PMid:24528749.
41. Ribeiro, J. S., Ferreira, M. M. C., & Salva, T. J. G. (2011). Chemometric models for the quantitative descriptive sensory analysis of Arabica coffee beverages using near infrared spectroscopy. *Talanta*, *83*(5), 1352-1358. http://doi.org/10.1016/j.talanta.2010.11.001. PMid:21238720.
42. Craig, A. P., Botelho, B. G., Oliveira, L. S., & Franca, A. S. (2018). Mid infrared spectroscopy and chemometrics as tools for the classification of roasted coffees by cup quality. *Food Chemistry*, *245*, 1052-1061. http://doi.org/10.1016/j.foodchem.2017.11.066. PMid:29287322.
43. Barrios-Rodríguez, Y., Collazos-Escobar, G. A., & Gutiérrez-Guzmán, N. (2021). ATR-FTIR for characterizing and differentiating dried and ground coffee cherry pulp of different varieties (*Coffea arabica* L.). *Engenharia Agrícola*, *41*(1), 70-77. http://doi.org/10.1590/1809-4430-eng.agric.v41n1p70-77/2021.
44. Chieng, B. W., Ibrahim, N. A., Yunus, W. M. Z. W., & Hussein, M. Z. (2013). Poly(lactic acid)/poly(ethylene glycol) polymer nanocomposites: effects of graphene nanoplatelets. *Polymers*, *6*(1), 93-104. http://doi.org/10.3390/polym6010093.
45. Wang, N., Zhang, X., Ma, X., & Fang, J. (2008). Influence of carbon black on the properties of plasticized poly (lactic acid) composites. *Polymer Degradation & Stability*, *93*(6), 1044-1052. http://doi.org/10.1016/j.polymdegradstab.2008.03.023.
46. Angin, N., Caylak, S., Ertas, M., & Cavdar, A. D. (2022). Effect of alkyl ketene dimer on chemical and thermal properties of polylactic acid (PLA) hybrid composites. *Sustainable Materials and Technologies*, *32*, e00386. http://doi.org/10.1016/j.susmat.2021.e00386.
47. Santos, R. S., Silveira, P. H. P. M., Bastos, B. C., Conceição, M. N., Ribeiro, R. C. C., & Bastos, D. C. (2023). Development of environmentally ecofriendly composites based on polypropylene/Bahia Beige Waste: effect of reinforcement content on physical, mechanical, chemical, and microstructural properties. *Recent Progress in Materials*, *5*(3), 27. http://doi.org/10.21926/rpm.2303027.

48. Bakshi, P., Pappu, A., Bharti, D. K., & Patidar, R. (2021). Accelerated weathering performance of injection moulded PP and LDPE composites reinforced with calcium rich waste resources. *Polymer Degradation & Stability*, *192*, 109694. http://doi.org/10.1016/j.polymdegradstab.2021.109694.

49. Ou, R., Xie, Y., Wolcott, M. P., Sui, S., & Wang, Q. (2014). Morphology, mechanical properties, and dimensional stability of wood particle/high density polyethylene composites: effect of removal of wood cell wall composition. *Materials & Design*, *58*, 339-345. http://doi.org/10.1016/j.matdes.2014.02.018.

50. Silveira, P. H. P. M., Conceição, M. N., Pina, D. N., Paes, P. A. M., Monteiro, S. N., Tapanes, N. L. C. O., Ribeiro, R. C. C., & Bastos, D. C. (2024). Impact of different mineral reinforcements on HDPE COMPOSITES: effects of melt flow index and particle size on physical and mechanical properties. *Polymers*, *16*(14), 2063. http://doi.org/10.3390/polym16142063. PMid:39065380.

51. Borsoi, C., Berwig, K. H., Scienza, L. C., Zoppas, B. C. D. A., Brandalise, R. N., & Zattera, A. J. (2014). Behavior in simulated soil of recycled expanded polystyrene/waste cotton composites. *Materials Research*, *17*(1), 275-283. http://doi.org/10.1590/S1516-14392013005000167.

52. Coelho, K. V. S., Líbano, E. V. D. G., Ramos Filho, F. G., Santos, S. F., Pereira, P. S. C., & Bastos, D. C. (2021). Development of wood plastic composite with reduced water absorption. *International Journal of Developmental Research*, *11*(2), 44547-44551.

53. Kadea, S., Kittikorn, T., & Hedthong, R. (2024). Sustainable laminate biocomposite of wood pulp/PLA with modified PVA-MFC compatibilizer: weathering resistance and biodegradation in soil. *Industrial Crops and Products*, *218*, 118913. http://doi.org/10.1016/j.indcrop.2024.118913.

54. Siakeng, R., Jawaid, M., Asim, M., & Siengchin, S. (2020). Accelerated weathering and soil burial effect on biodegradability, colour and texture of coir/pineapple leaf fibres/PLA biocomposites. *Polymers*, *12*(2), 458. http://doi.org/10.3390/polym12020458. PMid:32079111.

55. Jaramillo, L. Y., Vásquez-Rendón, M., Upegui, S., Posada, J. C., & Romero-Sáez, M. (2021). Polyethylene-coffee husk eco-composites for production of value-added consumer products. *Sustainable Environment Research*, *31*(1), 34. http://doi.org/10.1186/s42834-021-00107-6.

56. Petinakis, E., Yu, L., Simon, G. P., Dai, X. J., Chen, Z., & Dean, K. (2014). *Interfacial adhesion in natural fiber-reinforced polymer composites.* In V. K. Thakur (Ed.), *Lignocellulosic polymer composites: processing, characterization, and properties* (pp. 17-39). Massachusetts: Scrivener Publishing LLC. http://doi.org/10.1002/9781118773949.ch2.

57. Almeida, P. O., Gerardo, C. F., de Leão, A. G., França, S. C. A., Santos, S. F., & Bastos, D. C. (2021). Sustainable composites based on recycled high-density polyethylene/mica. *Materials Research*, *24*(2), e20200418. http://doi.org/10.1590/1980-5373-mr-2020-0418.

58. Silveira, P. H. P. M., Santos, M. C. C., Chaves, Y. S., Ribeiro, M. P., Marchi, B. Z., Monteiro, S. N., Gomes, A. V., Tapanes, N. L. C. O., Pereira, P. S. C., & Bastos, D. C. (2023). Characterization of thermo-mechanical and chemical properties of polypropylene/hemp fiber biocomposites: impact of maleic anhydride compatibilizer and fiber content. *Polymers*, *15*(15), 3271. http://doi.org/10.3390/polym15153271. PMid:37571165.

59. Acosta, A. P., Amico, S. C., Delucis, R. A., Missio, A. L., Rodrigues, M. B. B., Ribeiro, A. C. R., Goularte, M. P., & Gatto, D. A. (2024). Surface analysis of different wood polymer composites exposed to artificial weathering. *Journal of Wood Chemistry and Technology*, *44*(2), 88-101. http://doi.org/10.1080/02773813.2023.2299814.

60. Melgosa, M., Ruiz-López, J., Li, C., García, P. A., Della Bona, A., & Pérez, M. M. (2020). Color inconstancy of natural teeth measured under white light-emitting diode illuminants. *Dental Materials*, *36*(12), 1680-1690. http://doi.org/10.1016/j.dental.2020.10.001. PMid:33172605.

61. Mitchell, M. K., & Hirt, D. E. (2015). Degradation of PLA fibers at elevated temperature and humidity. *Polymer Engineering and Science*, *55*(7), 1652-1660. http://doi.org/10.1002/pen.24003.

62. Vasile, C., Pamfil, D., Rapa, M., Darie-Nit, R. N., Mitelut, A. C., Popa, E. E., Popescu, P. A., Draghici, M. C., & Popa, M. E. (2018). Study of the soil burial degradation of some PLA/CS biocomposites. *Composite B Engineering*, *142*, 251-262. http://doi.org/10.1016/j.compositesb.2018.01.026.

Received: Feb. 26, 2024
Revised: July 11, 2024
Accepted: July 17, 2024